Supporting information

Temperature-dependent Structural and Spectroscopic Studies of $(Bi_{1-x}Fe_x)FeO_3$

Andrea Kirsch[a,b], M. Mangir Murshed[a,b*], Melanie J. Kirkham[c], Ashfia Huq[c], F. Jochen Litterst[d], Thorsten M. Gesing[a,b]

[a]University of Bremen, Institute of Inorganic Chemistry and Crystallography, Leobener Straße 7, D-28359, Bremen, Germany

[b]University of Bremen, MAPEX center for materials and processes, Bibliothekstraße 1, D-28359 Bremen, Germany

[c]Chemical and Engineering Materials Division, Oak Ridge National Laboratory, Oak Ridge, Tennessee 37831, USA

[d]Institute for Condensed Matter Physics, Technische Universität Braunschweig, Mendelssohnstr. 3, D-38106 Braunschweig, Germany

*Corresponding author; e-mail address: murshed@uni-bremen.de; phone: +49 (0)421 218 63144; fax: +49 (0)421 218 63144

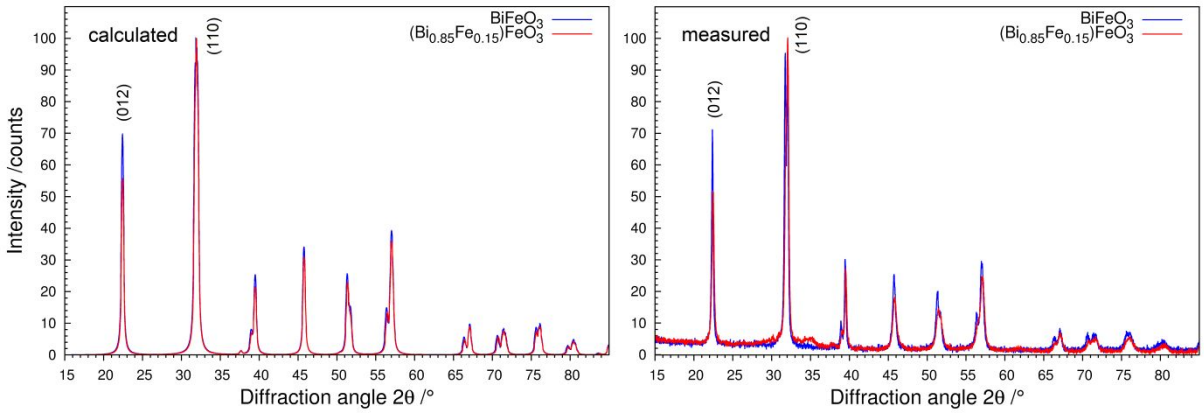

Figure 1S. Simulated (left panel) and measured (right panel) X-ray powder patterns of $BiFeO_3$ and $(Bi_{1-x}Fe_x)FeO_3$. The program POWDER CELL[1] was used for simulations and the data was normalized to the (*110*) reflection.

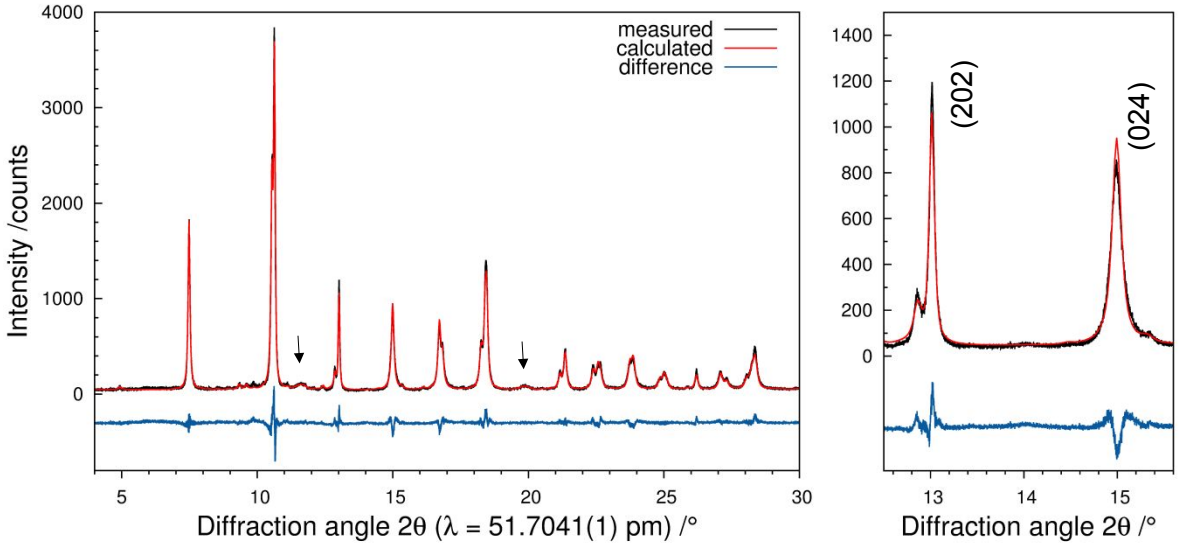

Figure 2S. Rietveld patterns of $(Bi_{0.85}Fe_{0.15})FeO_3$ for the synchrotron X-ray data (APS). The magnification (right) shows the huge anisotropy of two neighbouring reflections.

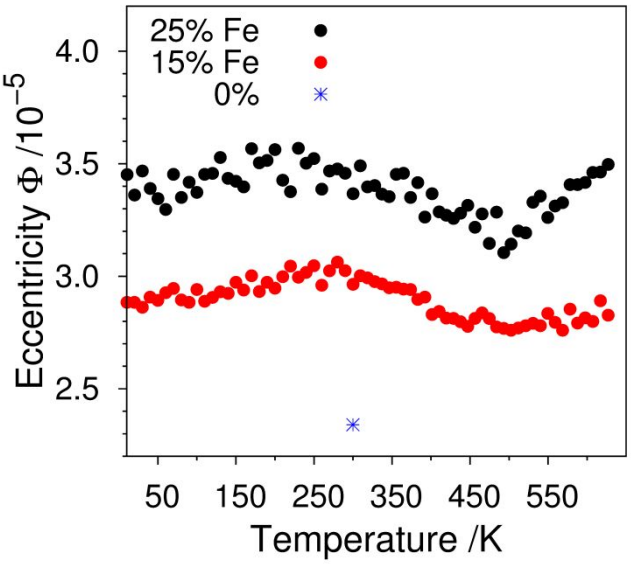

Figure 3S. Temperature-dependent Wang-Liebau eccentricity (WLE) parameter of the $(Bi/Fe)O_6$ octahedra of $(Bi_{1-x}Fe_x)FeO_3$ and room-temperature value of the BiO_6 octahedra of $BiFeO_3$.

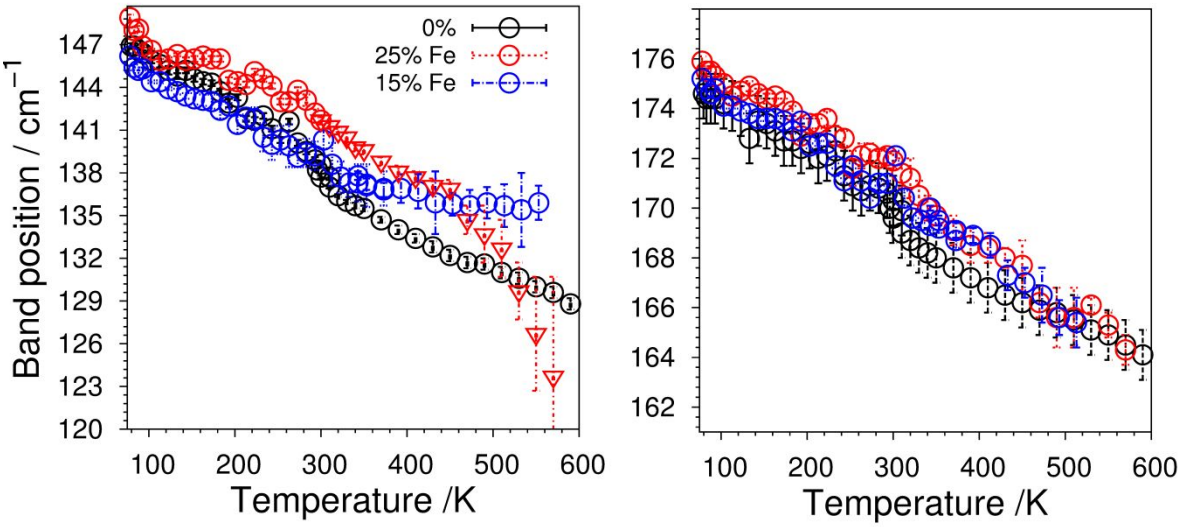

Figure 4S. Temperature-dependent band positions of the E(TO2) and A_1(TO1) modes of $(Bi_{1-x}Fe_x)FeO_3$ for x = 0, 0.15 and 0.25.

Table 1S. Raman frequency of mode E(TO2) and A_1(TO1) at 0 K (obtained from extrapolation of the low-temperature data) along with respective Grüneisen parameter (γ_i).

Compound	E(TO2)		A_1(TO1)	
	$\omega_{i,0}$ /cm^{-1}	γ_i	$\omega_{i,0}$ /cm^{-1}	γ_i
$BiFeO_3$[2]	135.7	1.94	168.9	1.74
$(Bi_{0.85}Fe_{0.15})FeO_3$	141.7(1)	8.9(3)	171.3	4.6(3)
$(Bi_{0.75}Fe_{0.25})FeO_3$	140.9(1)	6.8(2)	171.3	4.1(2)

Table 2S. Elastic coefficients (C_{ij}) and bulk moduli of $BiFeO_3$.

Method	C_{11}	C_{12}	C_{13}	C_{14}	C_{33}	C_{44}	C_{66}	B_R	B_V	B_H	B_0	Ref.
IXA	207(5)	-	-	-	159(4)	30(1)	42(1)	-	-	-	-	[3]
LDA	249	-	75	9	160	44	49	-	-	-	-	[3]
GGA	203	117	50	23	129	31	43	96	108	102	-	[4]
GGA + U (3 V)	213	111	49	19	139	39	51	99	109	104	-	[4]
GGA + (U 6 V)	222	110	50	16	150	49	56	104	113	108	-	[4]
XRPD	-	-	-	-	-	-	-	-	-	-	97.3(7)	[5]
XRPD	-	-	-	-	-	-	-	-	-	-	75(15)	[6]

IXA = Inelastic X-ray, B_0 = Bulk modulus (Reuss), B_R = Bulk modulus (Reuss), B_V = Bulk modulus (Voigt), B_H = Bulk modulus (Hill average)

Reference

(1) Kraus, W.; Nolze, G. *POWDER CELL*– a Program for the Representation and Manipulation of Crystal Structures and Calculation of the Resulting X-ray Powder Patterns. *J. Appl. Crystallogr.* **1996**, *29*, 301–303.

(2) Yang, Y.; Sun, J. Y.; Zhu, K.; Liu, Y. L.; Chen, J.; Xing, X. R. Raman Study of $BiFeO_3$ with Different Excitation Wavelengths. *Phys. B Condens. Matter* **2009**, *404*, 171–174.

(3) Borissenko, E.; Goffinet, M.; Bosak, A.; Rovillain, P.; Cazayous, M.; Colson, D.; Ghosez, P.; Krisch, M. Lattice Dynamics of Multiferroic $BiFeO_3$ Studied by Inelastic X-ray Scattering. *J. Phys. Condens. Matter* **2013**, *25*, 102201.

(4) Shang, S. L.; Sheng, G.; Wang, Y.; Chen, L. Q.; Liu, Z. K. Elastic Properties of Cubic and Rhombohedral BiFeO3 from First-principles Calculations. *Phys. Rev. B.* **2009**, *80*, 52102.

(5) Zhu, J. L.; Feng, S. M.; Wang, L. J.; Jin, C. Q.; Wang, X. H.; Li, L. T.; Li, Y. C.; Li, X. D.; Liu, J. Structural Stability of Multiferroic $BiFeO_3$. *High Press. Res.* **2010**, *30*, 265–272.
(6) Gavriliuk, A. G.; Struzhkin, V. V.; Lyubutin, I. S.; Ovchinnikov, S. G.; Hu, M. Y.; Chow, P. Another Mechanism for the Insulator-metal Transition Observed in Mott Insulators. *Phys. Rev. B,* **2008**, *77*, 155112.